THE JOURNAL OF PHYSICAL CHEMISTRY A

 VOLUME 111, NUMBER 45, NOVEMBER 15, 2007

ARTICLES

Computational Study of the Zr^{4+} Tetranuclear Polymer, $[Zr_4(OH)_8(H_2O)_{16}]^{8+}$

Niny Rao,[†] Marian N. Holerca,[‡] Michael L. Klein,[§] and Vojislava Pophristic*,[†]

Department of Chemistry & Biochemistry and the West Center for Computational Chemistry and Drug Design, University of the Sciences in Philadelphia, Philadelphia, Pennsylvania 19104, Colgate Palmolive Company, Global Technology Center, Piscataway, New Jersey 08854, and Center for Molecular Modeling and Department of Chemistry, University of Pennsylvania, Philadelphia, Pennsylvania 19104-6323

Received: May 7, 2007; In Final Form: July 22, 2007

The Zr^{4+} tetramer, $[Zr_4(OH)_8(H_2O)_{16}]^{8+}$, is thought to be the major component of the Zr^{4+} polymer system in aqueous solution, present as a dominant ionic cluster species compared to other Zr^{4+} clusters under various experimental conditions. Despite widespread applications of zirconium, the structure and dynamics of the tetramer in aqueous solution are not well understood. We conducted a combination of ab initio molecular dynamics and quantum mechanical studies in the gas phase and aqueous solution and related our results to the available experimental data to provide atom-level information on the behavior of this species in aqueous solution. Our simulations indicate that the tetramer structure is stable on the picosecond time scale in an aqueous environment and that it is of a planar form, comprising eight-coordinated Zr^{4+} ions with an antiprism/irregular dodecahedron ligand arrangement. In combination with our studies of Zr^{4+} dimer and trimer clusters, our results provide detailed geometrical information on structural motifs for building zirconium polymers and suggest a possible polymerization path.

I. Introduction

Understanding the chemistry and physicochemical properties of aqueous solutions of inorganic ions is of crucial importance for a variety of chemical problems in both basic and applied science. Solutions of a number of highly charged metal cations present an experimental challenge, because of the polymerization that occurs to different extents depending on pH, aging, temperature, and concentration. Computational chemistry methods provide a tool for circumventing some of these problems and have been shown to contribute important information about solution characteristics. We focus on solvation of the Zr^{4+} ion, because of a wide range of zirconium applications that call for a better understanding of its characteristics.

Upon contact with water, Zr^{4+} ions form a complex mixture of polynuclear species, with the composition depending on a combination of experimental conditions.[1−4] A number of experimental studies conducted over the past 5 decades[5−11] point to the zirconium tetramer, $[Zr_4(OH)_8(H_2O)_{16}]^{8+}$, as a major component of Zr^{4+} solutions, present in aqueous solutions along with a variety of other polymers. Despite the general scientific and industrial interest in this species (applications range from nuclear technology to antiperspirants),[3,12] there have been no computational studies of the zirconium tetramer that would provide atom-level information on its structure and dynamics in aqueous solution.

Ab initio molecular dynamics techniques, such as Car−Parrinello molecular dynamics (CPMD),[13] allow models of relatively small polymers (of the zirconium tetramer size) in

* Corresponding author. E-mail: v.pophri@usip.edu. Tel.: 215-596-8551. Fax: 215-596-5432.
[†] University of the Sciences in Philadelphia.
[‡] Colgate Palmolive Company
[§] University of Pennsylvania.

10.1021/jp0734880 CCC: $37.00
Published on Web 10/18/2007

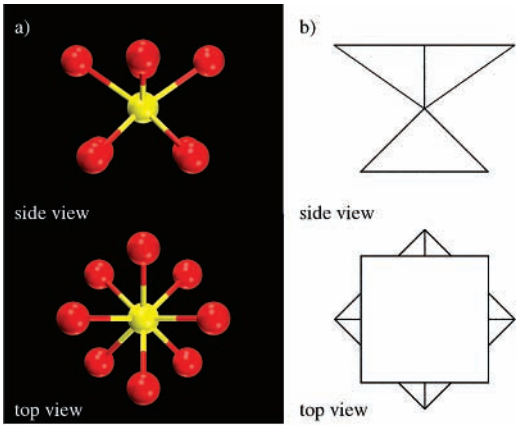

Figure 1. Square antiprism shape used as the building unit for the initial structure design of the tetramer. Two models (and two views) are shown. (a) Ball-and-stick model: lines represent bonds between the Zr^{4+} ion (yellow) and oxygen atoms (red) of OH and H_2O moieties. (b) Model represented by planes cornered by Zr^{4+} ion and oxygen atoms.

aqueous solution to be studied and important chemical processes such as bond breaking and formation, water deprotonation, species dynamics, and interactions between particles in solution to be observed. The advantage of the CPMD method with respect to classical molecular dynamics lies in the fact that the former does not employ empirically parametrized forces to govern atomic motion, but rather determines them "on the fly", from electronic structure calculations. In addition, the computational approach to studying systems that easily polymerize to yield various polynuclear species presents a key complement to experimental studies, because of the atomic level of insight and higher level of control of the system's composition and conditions. The usefulness and effectiveness of CPMD in small inorganic polymer studies has been demonstrated for a number of systems, such as aluminum hydroxide[14] and aluminum chlorohydrate.[15,16]

Herein, we focus on the stability and chemical behavior of the Zr^{4+} tetramer in aqueous solution. The structure of this species $[Zr_4(OH)_8(H_2O)_{16}Cl_8]$ was determined by early X-ray[5,6] and some later experiments.[7] X-ray scattering studies have shown that this species is the major form present in solutions.[6,11] Spectrophotometric[17] and ultracentrifugation[18] studies also suggest the presence of the tetramer, which has been confirmed by several recent publications.[8,9] We have obtained and characterized the gas-phase and solution structures of the tetramer using the CPMD approach and conducted an analysis of its stability and chemical behavior in aqueous solution.

II. Methodology

Within the CPMD[13] framework, we employ a Goedecker-type pseudopotential for zirconium (12 valence electrons)[19] and nonlocal norm-conserving soft pseudopotentials of Troullier−Martins type[20] for oxygen and hydrogen. Angular momentum components up to $l_{max} = 2$ were included for Zr and $l_{max} = 1$ for O. The BLYP exchange correlation functional was employed,[21,22] along with a plane-wave basis with a 70-Ry cutoff. Neutralizing background charge was used. All simulations were performed in a periodically repeating cubic box, with different sizes for the gas-phase and solution simulations (see below) and periodic boundary conditions.

The initial structure of the tetramer was constructed using its X-ray structure[5,6] and a square antiprism as the building unit (Figure 1), based on the 7−8 coordination of Zr^{4+} ion and our

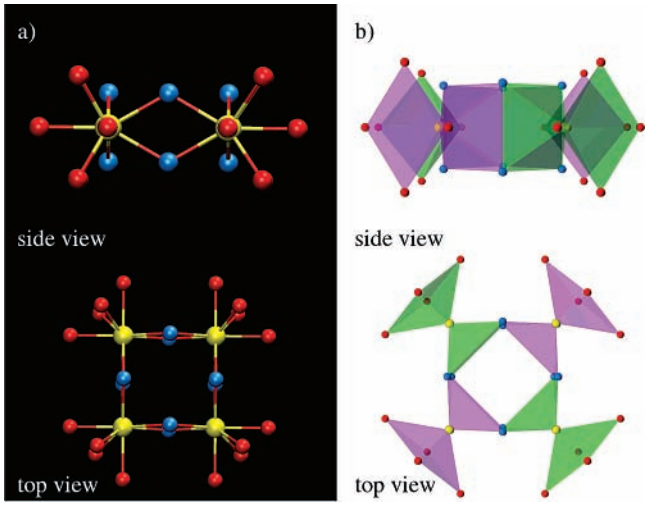

Figure 2. Initial structure of the tetramer. Pairs of Zr^{4+} ions are connected by two OH bridges each. (a) Ball-and-stick model. (b) Two square antiprism monomer units shown in different colors (green, purple) to facilitate viewing. Zr^{4+} ions, yellow; oxygen atoms in OH bridging groups, blue; oxygen atoms in H_2O molecules, red. Side and top views are shown. Hydrogen atoms omitted for clarity.

CPMD simulations of the Zr^{4+} ion in solution.[23] The minimum-energy geometry of the gas-phase structure was obtained by an initial relaxation at 300 K for >1 ps, followed by simulated annealing (scaling factor of 0.9998 for ionic velocities) and geometry optimization. The gas-phase simulation cell edge was 18.0 Å. In all calculations, classical equations of motion were integrated with the velocity Verlet algorithm with a time step of 0.1207 fs and a fictitious mass for the electronic degrees of freedom of $\mu = 500$ a.u.

After optimization by the CPMD code, the tetramer geometry was refined by BLYP[24,25] and B3LYP optimizations,[25,26] using the LanL2DZ basis set,[27] the size of the tetramer preventing higher-level optimizations. These optimizations were carried out with Gaussian 03.[28] Harmonic frequencies for the optimized geometries were calculated to ensure that they correspond to the local minima.

The optimized gas-phase structure was used as the starting geometry for the simulations in aqueous solution. The aqueous environment was modeled by a cubic box with a 16.0 Å edge and 108 H_2O molecules. The analysis of the system was performed based on the trajectory obtained from the ~10 ps CPMD simulation using a Nosé−Hoover chain thermostat (of length 4, with frequency 500 cm^{-1})[29−32] at 300 K.

III. Results

III.1. $[Zr_4(OH)_8(H_2O)_{16}]^{8+}$: Gas-Phase Structure. The initial tetramer geometry was designed following the X-ray structure of $Zr_4(OH)_8(H_2O)_{16}Cl_8$.[5] It consists of four Zr^{4+} ions, each eight-coordinated in a square antiprism fashion (Figure 2). These monomer units are connected by double OH bridges, thus making the coordination shell of each Zr^{4+} consist of four OH^- groups (within bridges, i.e., shared between adjacent Zr^{4+} ions) and four H_2O molecules, bound to Zr ions via oxygen atoms. The overall structure is planar with respect to the Zr ions, with Zr^{4+} ions in the corners of a square and OH bridges symmetrically arranged above and below the plane formed by four Zr^{4+} ions, equidistant from the Zr^{4+} ions that they connect.

This structure was allowed to relax in the gas phase at 300 K for >1 ps, followed by simulated annealing, which led to a stable structure with four Zr^{4+} ions in the corners of a square and oxygen atoms symmetrically arranged (both in the bridges

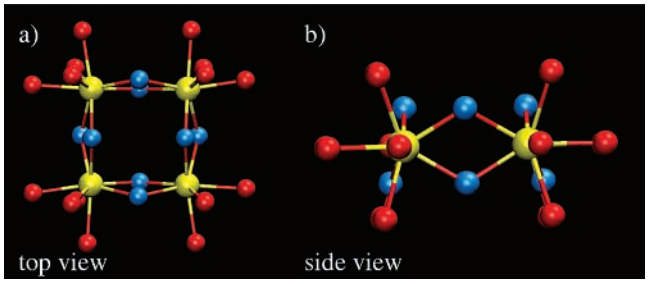

Figure 3. Optimized structure of the tetramer (gas phase). (a) Top view, showing the square arrangement of the four Zr ions. (b) Side view, showing the planarity of the zircounium ion and the OH bridge arrangement. Zr^{4+} ions, yellow; oxygen atoms in OH bridging groups, blue; oxygen atoms in H_2O molecules, red. Hydrogen atoms omitted for clarity.

TABLE 1: Optimized Geometry of the Zr^{4+} Tetramer, Obtained Using Different Computational Levels[a]

	BLYP/plane-wave basis	BLYP/ LanL2DZ	B3LYP/ LanL2DZ
	distance (Å)		
Zr−Zr	3.749−3.756	3.791	3.748
Zr−O_{OH}	2.183−2.224	2.202−2.242	2.183−2.218
Zr−O_{H_2O}	2.303−2.426	2.301−2.397	2.280−2.372
	angle (deg)		
Zr−Zr−Zr	89.88−90.15	89.99−90.00	89.99−90.01
O_{OH}−Zr−O_{OH}	62.58−62.96	62.16−62.60	62.53−62.82
Zr−O_{OH}−Zr	115.36−117.34	115.80−117.77	115.49−117.51
O_{OH}−Zr−O_{H_2O}(1)[b]	81.39−98.02	81.80−99.89	81.65−99.71
O_{OH}−Zr−O_{H_2O}(2)[c]	74.34−76.17	74.80−76.78	74.82−76.72
O_{H_2O}−Zr−O_{H_2O}[d]	70.51−73.83	70.61−72.73	70.35−72.72

[a] The optimized Zr tetramer has a square configuration, with two adjacent antiprism units joined along the edge defined by the two bridging OH groups. The four Zr^{4+} ions are in a planar configuration. There are four H_2O molecules surrounding each Zr ion; two of them lay on the plane defined by the Zr ions, and the other two are located above or below the plane. [b] O_{OH}−Zr−O_{H_2O}(1) refers to angles defined by hydroxyl O, Zr, and water O atoms, where water O atoms lie on the plane defined by the Zr ions. [c] O_{OH}−Zr−O_{H_2O}(2) refers to angles defined by hydroxyl O, Zr, and water O atoms located above or below the plane defined by Zr ions. [d] O_{H_2O}−Zr−O_{H_2O} refers to angles defined by the Zr ion and oxygen atoms of two water molecules bound to it.

and in the terminal H_2O molecules). The structure was subsequently optimized using BLYP/plane wave and BLYP/LanL2DZ and B3LYP/LanL2DZ procedures (Figure 3), with resulting geometrical parameters in close agreement between the two procedures (Table 1). Neither the change in the nature of the basis set (plane wave → LanL2DZ) nor the change in the computational level (BLYP → B3LYP) affects the geometrical parameters much, especially for the angles. The Zr−Zr distances are 3.7−3.8 Å, whereas the Zr−O distances are ∼2.2 Å for OH bridges and 2.3−2.4 Å for H_2O ligands. The gas-phase optimized tetramer retains the main geometrical features of the X-ray-determined solid-state structure: four Zr^{4+} ions are in one plane, with OH bridges and H_2O ligands surrounding any one of the Zr^{4+} ions highly symmetrically with respect to the groups surrounding the other three Zr^{4+} ions. Because of the spatial restrictions imposed by the bridges, the arrangements of H_2O ligands around two adjacent Zr^{4+} ions are eclipsed with respect to each other, as opposed to the minimum-energy structure of the dimer, which is staggered.[33] Otherwise, the tetramer bond lengths and angles agree well with those of the gas-phase dimer $[Zr_2(OH)_2(H_2O)_{12}{}^{6+}]$ optimized at the same level.[33]

Experimental data most often cited for the zirconium tetramer are derived from the characteristics of the zirconium oxychloride {$ZrOCl_2 \cdot 8H_2O$ or $[Zr_4(OH)_8(H_2O)_{16}]Cl_8 \cdot 12H_2O$} crystal structure, which was originally determined in 1956.[5] Since then, the species has been studied by various means, both in the solid state and in solution.[1−3,6,10,11,34] Our calculated gas-phase Zr−O distances agree with the solid-state data (2.13−2.37 Å),[5] as does the general position of the OH bridging groups (pairs arranged so that one OH group is above and the other is below the Zr plane). Geometrical parameters derived from EXAFS spectra on aqueous solutions of $ZrOCl_2 \cdot 8H_2O$, $ZrO(NO_3)_2 \cdot 2H_2O$, and $Zr(SO_4)_2 \cdot 4H_2O$ salts, which produce tetrameric species (reported Zr−Zr distances between adjacent ions are 3.3 and 3.6 Å depending on the nature of the anion and the age of the solution, whereas Zr−O distances are 2.2 Å),[10] are also in agreement with the values obtained here. The Zr−O distance also falls in the range of experimentally and computationally obtained values for related structures, such as the tetragonal crystalline ZrO_2 structure (2.09−2.44 Å),[35] solid-state but amorphous ZrO_2 (2.04−2.25 Å),[36] and a class of $Zr(OH)_n(H_2O)_m$ monomers (ab initio calculated values for gas-phase: Zr−O_{OH}, 1.9−2.2 Å; Zr−O_{H_2O}, 2.2−2.4 Å).[37] The Zr−Zr distance is, as expected, somewhat larger than in the monoclinic ZrO_2 structure (crystal structure data), which is 3.44−3.47 Å.[38]

III.2. $[Zr_4(OH)_8(H_2O)_{16}]^{8+}$: Solution Structure. The gas-phase-optimized tetramer was placed in a box (16.0 Å edge) with 108 water molecules and equilibrated for 10 ps. The results of the simulation are presented in Figures 4 and 5. The Zr−O and Zr−H radial distribution functions (Figure 4a,b) show that each of the four Zr ions is surrounded by four water molecules and four bridging hydroxide groups (coordination numbers are 8 and 12 for O and H, respectively). We observe no deprotonation of any of the terminal water molecules and no bound water molecules exchanging with the bulk or leaving the complex, as evident from the coordination numbers (12 for H) and the 0 value of the $g(r)$ functions between the first and second coordination shells for all four Zr^{4+} ions, respectively (Figure 4a,b). The distances between Zr ions (Figure 4c) oscillate around 3.66 Å, further confirming the stability of the species. The angular distribution function (Figure 4d) points to an irregular dodecahedron arrangement around the Zr ions, which, in an ideal case (ideal irregular dodecahedron), features peaks at 70°, 76°, 94°, 130°, and 143°. Some of the obtained peaks are in similar positions to those of the ideal antiprism (70°, 82°, 108°, 142°). Because of thermal distortions, as well as bending of certain Zr−O−Zr bonds stemming from the closed, circular square structure of the tetramer (Zr_1−O_{OH}−Zr_2−O_{OH}−Zr_3−O_{OH}−Zr_4−O_{OH}−Zr_1), we observe the following: (a) a wide peak at 60−90°, spanning the first three peaks of the irregular dodecahedron, and the first two peaks of the antiprism and (b) a wide peak at 130−150°, corresponding to the 130° and 143° irregular dodecahedron peaks as well as the 142° antiprism peak. One of the four Zr ions features a small peak at ∼110°, a characteristic of the antiprism geometry. Thus, as a consequence of the distortions of the ideal geometries, antiprism and irregular dodecahedron geometries are indistinguishable in the tetramer case.

Other geometrical features of the solvated cluster follow those observed by our gas-phase calculations, as well as by experimental studies in aqueous solution. The Zr−Zr radial distribution function (Figure 5a) features two peaks, one of which corresponds to the distance between the adjacent Zr ions, the other to the distance between Zr ions that are not directly bound to each other (3.6 and 5.1 Å, respectively). Our Zr−Zr radial distribution function is very close to the one observed by EXAFS experiments performed on the aqueous system (two sets

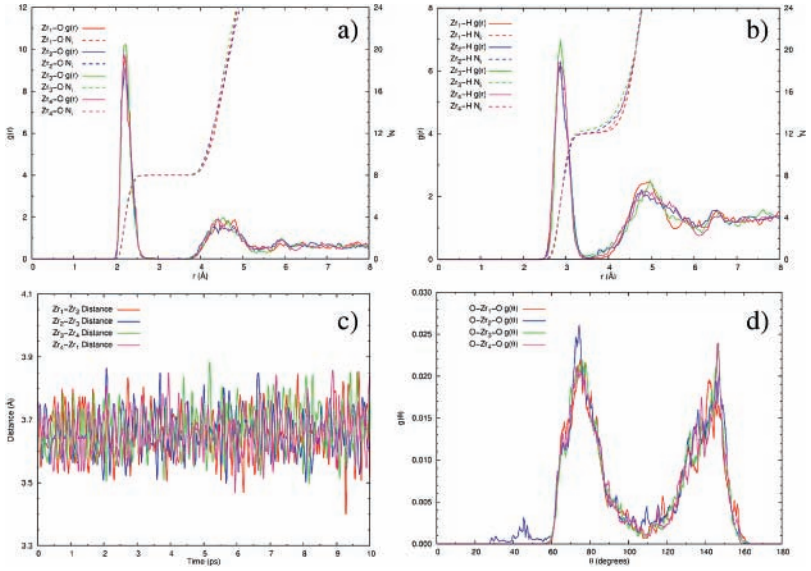

Figure 4. Zirconium tetramer in aqueous solution. (a) Zr−O radial distribution functions and corresponding running coordination number integrals for the four Zr^{4+} ions. (b) Zr−H radial distribution functions and corresponding running coordination number integrals for the four Zr^{4+} ions. (c) Zr−Zr distances for four pairs of adjacent Zr^{4+} ions. (d) Angular distribution function for the four Zr ions (O−Zr−O angle plotted), indicating the antiprism/irregular dodecahedron (indistinguishable in this case) arrangement of the coordinating oxygen atoms around each of the Zr ions.

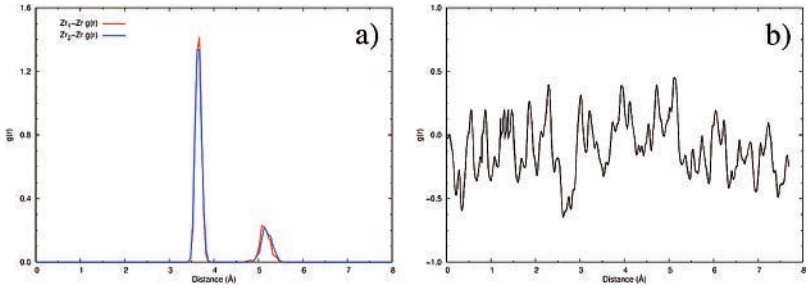

Figure 5. CPMD simulation of the zirconium tetramer in aqueous solution. (a) Zr−Zr radial distribution function. The plot shows that one of the Zr−Zr distances is $\sqrt{2}$ times larger than the other, indicating that the tetramer is a structure with square symmetry. (b) Distance of one Zr^{4+} ion from the plane defined by the other three Zr^{4+} ions. Small out-of-plane fluctuations (<0.5 Å) point to the stability and planarity of the aqueous solution structure.

of data reported because of dependence on the counteranion and aging, namely, 3.3 and 4.7 Å, and 3.6 Å and 5.1 Å, whereas the distances obtained from our simulations are 3.625 Å and 5.125 Å).[10] Such a set of distances confirms the square symmetry of the complex, given that the ratio of distances between the directly bound Zr ions (3.6 Å) and those that are diagonally related to each other (5.1 Å) is $\sqrt{2}$. On the time scale of the simulation, the tetramer appears to be planar: the departure of any one of the Zr ions from the plane formed by the other three Zr ions does not exceed 0.5 Å (Figure 5b).

IV. Discussion and Conclusions

The present CPMD simulations show that the Zr^{4+} tetramer cluster exists in aqueous solution as a stable structure, sharing common features mainly with the Zr^{4+} dimer. The basic structural motif observed by our studies of both the Zr^{4+} dimer and trimer clusters is present in the tetramer as well: the Zr^{4+} ion is eight-coordinated, which is consistent with general Zr^{4+} coordination.[1] The zirconium ion is surrounded by H_2O molecules and bridging hydroxide ions, with Zr−O bonds of $\sim$ 2.2 Å length. As opposed to the smaller clusters, in the case of the tetramer, we do not observe Zr−O bond breaking, i.e., exchange of the terminal, bound H_2O molecules with the bulk in either the gas-phase or solution simulations. The monomer unit takes an antiprism/irregular dodecahedron spatial arrangement that is somewhat distorted and cannot be uniquely assigned because of the strain imposed by the binding pattern between the units. Another structural motif is formed by the monomers bound by OH bridges, resulting in $Zr(OH)_2Zr$ units. This motif appears in both the dimer[33] and the tetramer species and has a consistent geometry when the two clusters are compared: the Zr−Zr distance is $\sim$3.8 Å, and the Zr−O_{OH} distance is $\sim$2.2 Å.

Although the $Zr(OH)_2Zr$ structural motif persists in going from the dimer to the tetramer, there is an interesting difference between the two: whereas one of the Zr ions in the dimer is seven-coordinated, all four Zr ions in the tetramer are eight-coordinated. In the course of a 10-ps simulation of the dimer in aqueous solution, we do not observe that the vacancy of the seven-coordinated Zr ion becomes filled by a water molecule from the bulk[33] (such behavior was observed in, e.g., the aluminum chlorohydrate Al_{13} cluster, using the same simulation method and on a similar time scale[15]). This observation points to a possible polymerization pathway from the dimer to the tetramer, which could occur by an attack of a dimer with a terminal OH group on a seven-coordinated Zr ion of another dimer. In such an arrangement, the seven-coordinated Zr ions could sterically accommodate an incoming OH group/bridge.[39] In addition, the comparison of the only trimer structure we were able to locate[33] and the trimer that can theoretically be extracted from the tetramer does not support a possible tetramer formation path via the trimer.

Our study of the tetramer in aqueous solution confirms what has been seen by X-ray studies in solid state: its aqueous solution form consists of four eight-coordinated Zr ions connected by double bridges and forming a roughly square and planar structure with respect to the Zr ions. The structure is stable on the scale of our simulation, with no tendency of either exchanging terminally bound water molecules with the bulk or breaking OH bridges. The excellent agreement of our results with the experimental data on the tetramer, together with our findings on the dimer and trimer,[33] provides a basis for new experiments to be designed and conducted that will shed more light on the aqueous chemistry of the Zr^{4+} ion.

Acknowledgment. This research was supported in part by the Petroleum Research Fund administered by the American Chemical Society (Grant 45086-G3), Colgate-Palmolive Company, and the National Science Foundation (Grant DMR05-20020). Computer time from Pittsburgh Supercomputing Center is greatly appreciated. N.R. and V.P. also acknowledge support from the H. O. West Foundation and NSF (CHE-0420556) and thank Dr. Z. Liu and Dr. E. Birnbaum for helpful discussions.

References and Notes

(1) Richens, D. T. *The Chemistry of Aqua Ions*; John Wiley & Sons: New York, 1997.

(2) Baes, C. F.; Mesmer, R. E. *The Hydrolysis of Cations*; John Wiley & Sons: New York, 1976.

(3) Rosenberg, A. H.; Fitzgerald, J. J. *Antiperspirants and Deodorants*; Marcel Dekker, Inc.: New York, 1999.

(4) Clearfield, A. *Rev. Pure Appl. Chem.* **1964**, *14*, 91−108.

(5) Clearfield, A.; Vaughan, P. A. *Acta Crystallogr.* **1956**, *9*, 555−558.

(6) Muha, G. M.; Vaughan, P. A. *J. Chem. Phys.* **1960**, *33*, 194−199.

(7) Mak, T. C. W. *Can. J. Chem.* **1968**, *46*, 3491.

(8) Ekberg, C.; Kallvenius, G.; Albinsson, Y.; Brown, P. L. *J. Solution Chem.* **2004**, *33*, 47−79.

(9) Veyland, A.; Dupont, L.; Pierrard, J. C.; Rimbault, J.; Aplincourt, M. *Eur. J. Inorg. Chem.* **1998**, 1765−1770.

(10) Kanazhevskii, V.; Novgorodov, B. N.; Shmachkova, V. P.; Kotsarenko, N. S.; Kriventsov, V. V.; Kochubey, D. I. *Mendeleev Commun. Elec. Version* **2001**, 1−2.

(11) Aberg, M. *Acta Chem. Scand. A: Phys. Inorg. Chem.* **1977**, *31*, 171−181.

(12) Northrup, C. J. M. J. Immobilization of U.S. defense nuclear wastes using the SYNROC process. In *Scientific Basis for Nuclear Waste Managment*; Plenum Press: New York, 1979; Vol. 2, p 265.

(13) Car, R.; Parrinello, M. *Phys. Rev. Lett.* **1985**, *55*, 2471−2474.

(14) Sillanpaa, A. J.; Paivarinta, J. T.; Hotokka, M. J.; Rosenholm, J. B.; Laasonen, K. E. *J. Phys. Chem. A* **2001**, *105*, 10111−10122.

(15) Pophristic, V.; Balagurusamy, V. S. K.; Klein, M. L. *Phys. Chem. Chem. Phys.* **2004**, *6*, 919−923.

(16) Pophristic, V.; Klein, M. L.; Holerca, M. N. *J. Phys. Chem. A* **2004**, *108*, 113−120.

(17) Zielen, A. J.; Connick, R. E. *J. Am. Chem. Soc.* **1956**, *78*, 5769.

(18) Johnson, J. S.; Kraus, K. A. *J. Am. Chem. Soc.* **1956**, *78*, 3937−3943.

(19) Goedecker, S.; Teter, M.; Hutter, J. *Phys. Rev. B* **1996**, *54*, 1703−1710.

(20) Troullier, N.; Martins, J. L. *Phys. Rev. B* **1991**, *43*, 1993.

(21) Becke, A. D. *Phys. Rev. A* **1988**, *38*, 3098.

(22) Lee, C.; Yang, W.; Parr, R. G. *Phys. Rev. B* **1988**, *37*, 785.

(23) The solvation of Zr^{4+} ion will be addressed in a separate publication.

(24) Becke, A. D. *Phys. Rev. A* **1988**, *38*, 3098−3100.

(25) Lee, C. T.; Yang, W. T.; Parr, R. G. *Phys. Rev. B* **1988**, *37*, 785−789.

(26) Becke, A. D. *J. Chem. Phys.* **1993**, *98*, 1372.

(27) Hay, P. J.; Wadt, W. R. *J. Chem. Phys.* **1985**, *82*, 270−283.

(28) Frisch, M. J. T., G. W.; Schlegel, H. B.; Scuseria, G. E.; Robb, M. A.; Cheeseman, J. R.; Montgomery, J. A., Jr.; Vreven, T.; Kudin, K. N.; Burant, J. C.; Millam, J. M.; Iyengar, S. S.; Tomasi, J.; Barone, V.; Mennucci, B.; Cossi, M.; Scalmani, G.; Rega, N.; Petersson, G. A.; Nakatsuji, H.; Hada, M.; Ehara, M.; Toyota, K.; Fukuda, R.; Hasegawa, J.; Ishida, M.; Nakajima, T.; Honda, Y.; Kitao, O.; Nakai, H.; Klene, M.; Li, X.; Knox, J. E.; Hratchian, H. P.; Cross, J. B.; Bakken, V.; Adamo, C.; Jaramillo, J.; Gomperts, R.; Stratmann, R. E.; Yazyev, O.; Austin, A. J.; Cammi, R.; Pomelli, C.; Ochterski, J. W.; Ayala, P. Y.; Morokuma, K.; Voth, G. A.; Salvador, P.; Dannenberg, J. J.; Zakrzewski, V. G.; Dapprich, S.; Daniels, A. D.; Strain, M. C.; Farkas, O.; Malick, D. K.; Rabuck, A. D.; Raghavachari, K.; Foresman, J. B.; Ortiz, J. V.; Cui, Q.; Baboul, A. G.; Clifford, S.; Cioslowski, J.; Stefanov, B. B.; Liu, G.; Liashenko, A.; Piskorz, P.; Komaromi, I.; Martin, R. L.; Fox, D. J.; Keith, T.; Al-Laham, M. A.; Peng, C. Y.; Nanayakkara, A.; Challacombe, M.; Gill, P. M. W.; Johnson, B.; Chen, W.; Wong, M. W.; Gonzalez, C.; Pople, J. A. *Gaussian 03*; Gaussian, Inc.: Pittsburgh, PA, 2004.

(29) Martyna, G. J.; Klein, M. L.; Tuckerman, M. *J. Chem. Phys.* **1992**, *97*, 2635−2643.

(30) Nose, S. *J. Chem Phys.* **1984**, *81*, 511.

(31) Nose, S. *Mol. Phys.* **1984**, *52*, 255.

(32) Hoover, W. G. *Phys. Rev. A* **1985**, *31*, 1695.

(33) Rao, N.; Holerca, M. N.; Pophristic, V. *J. Chem. Theory Comput.* **2007**, in press.

(34) Zielen, A. J. Report UCRL-2268; University of California Radiation Laboratory, Berkeley, CA, 1953.

(35) Safonov, A. A.; Bagatur'yants, A. A.; Korkin, A. A. *Microelectron. Eng.* **2003**, *69*, 629−632.

(36) Zhao, X.; Ceresoli, D.; Vanderbilt, D. *Phys. Rev. B* **2005**, *71*, 085107.

(37) Chen, S. G.; Yin, Y. S.; Wang, D. P. *J. Mol. Struct.* **2004**, *690*, 181−187.

(38) Foschini, C. R.; Filho, O. T.; Juiz, S. A.; Souza, A. G.; Oliveira, J. B. L.; Longo, E.; Leite, E. R.; Paskocimas, C. A.; Varela, J. A. *J. Mater. Sci.* **2004**, *39*, 1935−1941.

(39) This problem will be addressed in a future publication.